Uncertainty in hydrological modelling of climate change impacts in four Norwegian catchments

Deborah Lawrence and Ingjerd Haddeland

ABSTRACT

Projections for the hydrological impacts of climate change are necessarily reliant on a chain of models for which numerous alternative models and approaches are available. Many of these alternatives produce dissimilar results which can undermine their use in practical applications due to these differences. A methodology for developing climate change impact projections and for representing the range of model outcomes is demonstrated based on the application of a hydrological model with input data from six regional climate scenarios, which have been further adjusted to match local conditions. Multiple best-fit hydrological model parameter sets are also used so that hydrological parameter uncertainty is included in the analysis. The methodology is applied to consider projected changes in the average annual maximum daily mean runoff in four catchments (Flaksvatn, Viksvatn, Masi and Nybergsund) which are characterised by regional differences in seasonal flow regimes. For catchments where rainfall makes the predominant contribution to annual maximum flows, hydrological parameter uncertainty is significant relative to other uncertainty sources. Parameter uncertainty is less important in catchments where spring snowmelt dominates the generation of maximum flows. In this case, differences between climate scenarios and methods for adjusting climate model output to local conditions dominate uncertainty.

Key words | climate scenarios, hydrological model uncertainty, mean annual flood, parameter optimisation

Deborah Lawrence (corresponding author)
Ingjerd Haddeland
Hydrological Modelling Section,
Norwegian Water Resources and Energy Directorate (NVE),
PO Box 5091, Majorstua N-0301, Oslo,
Norway
E-mail: *dela@nve.no*

INTRODUCTION

The potential impacts of climate change on runoff have significant implications for the optimisation of future hydropower production capacity, for the development of flood hazard maps and flood risk management plans, and for the assessment of reservoir dam safety throughout the Nordic region. Analyses of possible future changes in runoff are necessarily reliant on the application of a cascade of models, commencing with a global climate model (GCM) run under a particular greenhouse gas emissions scenario and dynamically downscaled to a regional scale using a regional climate model (RCM). To derive daily data of a quality suitable for catchment-scale modelling, precipitation and temperature output time series from RCM models are often further adjusted to improve their agreement with local observations. At each step in this model chain, one or more alternative models may be available and the various alternatives can produce differing results. In addition, different hydrological models, as well as different parameter sets for a given hydrological model, may generate dissimilar results. The end product of an impact analysis is, therefore, often a range of possible outcomes, rather than a 'one-number' estimate for a catchment. This array of results needs to be presented and evaluated in a manner that conveys the expected changes in runoff, the range of the projected outcomes, and the factors contributing to that range, if the results are to be useful in decision making and planning.

The use of multiple input datasets derived from alternative climate scenarios has become both a fairly common and a recommended practice in studies of climate change

doi: 10.2166/nh.2011.010

impacts. Several previous studies have considered the array of results obtained from hydrological models forced with input data derived from different emission scenarios, GCMs or RCMs (e.g. Arnell 1999; Prudhomme *et al.* 2003; Salathé 2005; Graham *et al.* 2007; Minville *et al.* 2008). The availability of various methods for downscaling or bias correcting results to a scale suitable for hydrological simulations has also led to numerous published comparisons (e.g. Salathé 2003; Wood *et al.* 2004; Diaz-Nieto & Wilby 2005; see also the review by Fowler *et al.* 2007). The focus in much previous work on hydrological impacts of climate change has been on uncertainty associated with the input data to a hydrological model, rather than arising from the hydrological model itself. Steele-Dunne *et al.* (2008) have, however, considered multiple hydrological model parameter sets in evaluating climate change impacts derived from a single input climate scenario, and Schaefli *et al.* (2007) have used distributions of parameters derived during hydrological model calibration, together with a range of climate scenarios and linked models. Kriaučiūnienė *et al.* (2009) have considered a range of global climate model datasets and calibrated hydrological model parameter sets to explore the sensitivity of river runoff to uncertainties introduced by differences in input data and in model parameters. A few of the more recent studies which have considered uncertainty arising from both input data and other sources have applied a Monte Carlo sampling approach within a Bayesian framework, such as demonstrated by New & Hulme (2000), to generate probability distribution functions to represent the full range of model results. In particular, Wilby & Harris (2006) use this methodology in their impact analysis of low flows which combines results from scenarios from different GCMs, RCMs, emission scenarios, downscaling techniques, as well as hydrological model parameters and model structure. In their application, cumulative distribution functions for the full range of model results and for individual uncertainty sources are constructed, and comparisons between various factors contributing to the uncertainty represented by the ensemble range are made.

The purpose of this paper is to present an example of the methodology proposed by Wilby & Harris (2006), as applied to an analysis of projected changes in the average annual maximum daily mean runoff in four example catchments in Norway. Climate input data for hydrological model forcing are derived from two GCMs run under two greenhouse gas emission scenarios, dynamically downscaled using a single RCM. This RCM output was further adjusted to local observation stations using two alternative techniques in previous work published by Beldring *et al.* (2008). Those downscaled climate scenarios were here used as input to 150 best-fit parameter sets for hydrological models for the four example catchments. Uncertainties introduced by the choice of emission scenario, climate model, and hydrological model parameter set are accordingly considered in this analysis, and their relative contributions to the range of results are compared between the catchments.

METHODOLOGY AND MODEL APPLICATION

Study catchments

Catchment-scale analysis of climate change impacts on daily streamflow generally requires the application of a hydrological model for a more detailed estimation of the water balance than is currently available from regional climate modelling. The HBV (Hydrologiska Byråns avdeling for Vattenbalans; 'Hydrological Bureau for Water Balance') hydrological model (Bergström 1976, 1995) has been used extensively within the Nordic region since it was first developed in the 1970s for catchment-scale rainfall–runoff modelling. During the past decade, it has been applied in modelling the hydrological impacts of climate change (e.g. Bergström *et al.* 2001). In spite of HBV's limited physical descriptions, calibrated HBV models tend to perform well (Lindström *et al.* 1997) and require only daily precipitation and temperature as input climatological data. For operational purposes, this is a significant advantage over more detailed physical models, as model applications are not so severely limited by data availability. In the work presented here, the 'Nordic' version of the HBV model (Sælthun 1996) was applied to the four catchments illustrated in Figure 1. Catchment properties, including catchment area, elevation, land cover and geology, are given in Table 1, together with the average annual precipitation and runoff for the catchment. The catchment properties (excluding

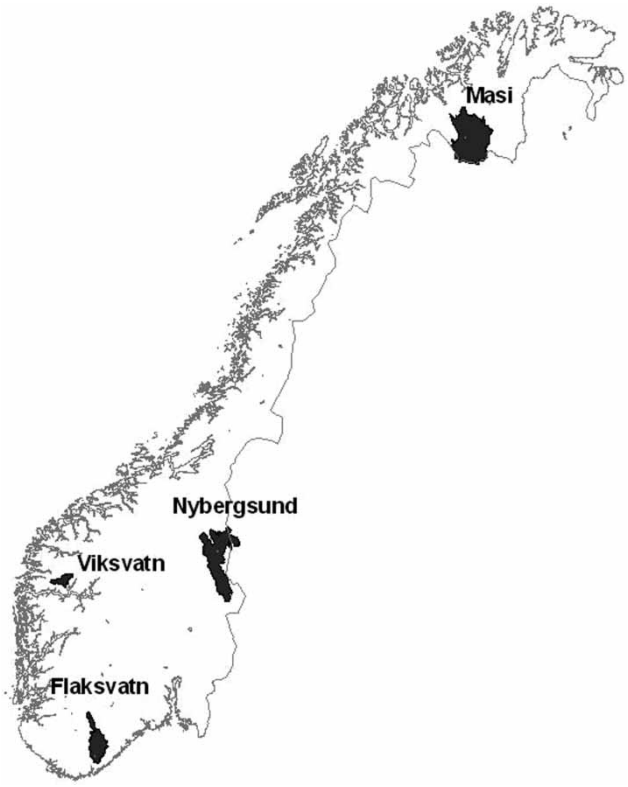

Figure 1 | Catchment locations.

geology) were extracted from raster datasets with a 25×25 m grid cell size, derived from 1:50,000 mapping. The dominant surface and bedrock geology were determined by visual inspection of the corresponding 1:50,000 maps for individual regions, relative to the catchment boundaries. Average annual precipitation for the period (1961–1990) was extracted from 1 by 1 km gridded data for Norway prepared by the Norwegian Meteorological Institute. Average annual runoff was estimated from observed daily runoff in the catchments. In the case of Masi, observed runoff data are only available from 1966, so the reported value reflects the period (1966–1990). The estimated percentage of the runoff derived from snowmelt was obtained from previous applications of the HBV model to these catchments.

Flaksvatn and Viksvatn are the smaller of the four catchments and are located in regions with pronounced topography. Both of these catchments receive significantly larger volumes of precipitation than the more inland (Nybergsund) and the more northern (Masi) catchments. This is also reflected in the differences in the average annual runoff, with the annual runoff in Viksvatn being more than five times that found in Masi. Both Masi and Nybergsund have annual flow regimes generally dominated by the spring snowmelt, as reflected in the estimated percentage of runoff derived from snowmelt. The elevation range and, particularly, the average catchment gradient is larger in Viksvatn and Flaksvatn than in Masi and Nybergsund, with Masi having the most subdued topography of the four. Due to their relative steepness and to their smaller catchment areas, the hydrologic response in Flaksvatn and Viksvatn is much more rapid than in the two larger catchments. In the smallest and steepest catchment, Viksvatn, the observed time lag between the onset of precipitation and peak discharge is typically of the order of 1.5 to 3 days for events of the magnitude of the mean annual flood. All four catchments are subjected to either zero or minimal regulation (Petterson 2004), so that daily data from discharge gauging stations are appropriate for use in hydrological model calibration, without correcting for impounding reservoirs in the upstream area.

The land surface in the westernmost catchment, Viksvatn, is dominated by exposed bedrock and forested areas, whilst Flaksvatn has a predominant forest cover, except in the uppermost reaches of the catchment, where exposed bedrock is the dominant land surface type. The uppermost portion of the Viksvatn catchment is glaciated, representing approximately 5% of the total catchment area. Masi and Nybergsund also have significant forested areas and zones of bare rock, but are characterised by a higher percentage of marsh and bog. The surface geology in Flaksvatn and Viksvatn is dominated by the exposed crystalline rock, although local talus and landslide deposits are particularly present in Viksvatn. Both Masi and Nybergsund have morainal deposits in the upstream portions of the catchment, but are also otherwise dominated by exposed bedrock. The bedrock geology in the catchments largely comprises of metamorphosed basement rock, including gneiss, quartzite, arkose and greenstone. Intrusive and extrusive igneous materials, as well as sandstones, shales and phyllites are also locally present.

The four catchments have differing annual flow regimes, reflecting their characteristics and geographic locations. High flows in Masi, Nybergsund and Viksvatn occur principally in spring or early summer due to snowmelt, whereas Flaksvatn and to some extent Viksvatn are also subjected

Table 1 | Catchment characteristics

Catchment property	Viksvatn	Flaksvatn	Masi	Nybergsund
Catchment area (km^2)	507	1,777	5,626	4,420
Median elevation (m.a.s.l.)	841	354	451	780
Average annual precipitation (mm)	3239	1497	605	721
Average annual runoff (mm)	2626	1053	390	482
Estimated portion of runoff from snowmelt (%)	43	30	79	57
Elevation, 90% of hypsometric curve (m.a.s.l.)	1,258	741	595	1,002
Elevation, 10% of hypsometric curve (m.a.s.l.)	302	197	370	644
Land cover, % lake	10	9	9	10
Land cover, % glacier	5	0	0	0
Land cover, % forest	23	76	38	45
Land cover, % marsh, bog	1	9	18	13
Land cover, % bare rock	59	5	35	31
Land cover, % other	2	1	0	1
Predominant Quaternary geology (Source: NGU, Norges geologiske undersøkelse, 'Norway's Geological Survey'; N50 maps)	Localised talus and landslide deposits	Minor localised peat/ marsh deposits	Moraine and outwash; localised peat/marsh	Moraine in upper reaches; localised peat/marsh
Predominant bedrock geology (Source: NGU, N50 maps)	Granitic orthogneiss	Metasandstone, quartzite, granitic gneiss, amphibolite	Metaarkose, quartzite, greenstone, granite, local shale and mafic tuft	Feldspathic sandstone; quartzite in upper reaches; some granite, rhyolite in lower reaches

to autumn rainfall flooding, in addition to snowmelt floods, under current climatic conditions. Climate change impacts on high flows are expected to differ between the catchments (Beldring *et al*. 2008), largely as a response to projected increases in rainfall flooding and decreases in the spring snowmelt volume. Projections for 2071–2100 indicate an earlier snowmelt and reduced snow storage which would lead to a reduction in the magnitude of snowmelt floods in Nybergsund and Masi. In Viksvatn and Flaksvatn, an increase in both precipitation and the proportion of precipitation which falls as rain, would contribute to an increase in the magnitude of high flows, particularly those associated with autumn and winter rainfall.

Hydrological model calibration and validation

Hydrological models were calibrated and validated with respect to observed mean daily discharge in each of the catchments for the period 1961–1990, corresponding to the reference period for which downscaled climate scenarios (e.g. Beldring *et al*. 2008) were available for this analysis. The period 1970–1985 was used as the calibration period, and the remaining years were used for model validation. Observed mean daily discharge data is available for all of the catchments for the period 1961–1990, excepting Masi, where observations began in 1966. Therefore, all of the catchments are calibrated relative to a 15-year daily data record (1970–1985). The model fits in the three catchments, excepting Masi, were validated for the periods (1961–1969) and (1986–1990), representing a total of 15 years. The validation periods for Masi are (1966–1969) and (1986–1990) for a total of 9 years. A daily timestep was used for model calibration and validation, reflecting the temporal resolution of the input precipitation and temperature data available for driving the model. Observed precipitation and temperature data for the calibration and

validation periods were derived from local station data, interpolated and corrected for altitude differences using a gridded version of the HBV model (Beldring *et al.* 2003). The 'Nordic' version of the HBV model uses 10 equal area height zones for estimating snow storage in the catchment, and land cover type is also distributed by height zone.

Model calibration was based on the application of PEST (Model Independent Parameter Estimation and Uncertainty Analysis; Doherty 2004) parameter estimation routines. Parameter estimation with PEST provides a more efficient method for obtaining optimal model fits than does uniform random sampling, which can be time and resource consuming (Solomatine *et al.* 1999). A disadvantage of PEST, however, is that it is a local, rather than a global, optimisation routine, such that the final optimised parameter values may be dependent on the initial values selected (Kite & Kouwen 1992). This limitation can be overcome by using multiple initial parameter sets to ensure that model fits correspond to global, rather than local optima (Skahill & Doherty 2006). Accordingly, a three-step procedure was used to select and optimise a set of 150 best-fit model parameter sets for each catchment.

First, an initial parameter set was generated by uniform random sampling from the ranges for 15 HBV parameters given in Table 2. The ranges of parameter values displayed in Table 2 is similar to those applied in manual calibrations and reported in Sælthun (1996), with a few exceptions. In particular, the range of values used for PKORR and SKORR are larger than is normally expected for these factors which correct the rainfall and snowfall input to the hydrological model. These larger ranges were found to function better with the local optimisation procedure used in PEST, although the final calibrated values are within the traditional ranges for these parameters. This randomly selected initial parameter set was then tested in the HBV model, and model performance was assessed based on the Nash–Sutcliffe value for the calibration period. If the Nash–Sutcliffe value exceeded 0.25 in this initial test, the parameter set was retained and optimised using PEST routines. Parameter sets not achieving this initial threshold value were discarded and a new set of initial parameter values was selected and tested. This initial selection procedure was used in order to minimise the computational time devoted to optimising parameter sets which would never produce satisfactory model fits. On average, each initial parameter set which was retained represents the testing of between 10 and 100 random initial parameter sets.

Table 2 | HBV parameter ranges used in PEST optimisation

HBV parameter	Description	Range considered
BETA	Soil moisture parameter	1.0–4.0
CX	Degree day correction factor	1.0–5.0
FC	Field capacity – soil zone	50.0–500.0
KLZ	Recession constant – lower zone	0.001–0.1
KUZ1	Recession constant – upper zone 1	0.01–1.0
KUZ2	Recession constant – upper zone 2	0.1–1.0
PERC	Percolation – upper to lower zone	0.5–2.0
PGRD	Precipitation lapse rate	0.0–0.1
PKORR	Rainfall correction factor	0.8–3.0
SKORR	Snowfall correction factor	1.0–3.0
TS	Threshold temp. for snowmelt	–1.0–2.0
TX	Threshold temp. for rain/snow	–1.0–2.0
TTGD	Temp. lapse rate – clear days	–1.0 to –0.5
TVGD	Temp. lapse rate during precip.	–0.7 to –0.3
UZ1	Threshold for quick runoff	10.0–00.0

Secondly, between 160 and 200 'acceptable' initial parameter sets were optimised for each catchment, with optimisation being performed so as to minimise two factors: (1) the difference between the observed and simulated daily discharge values for the calibration period; and (2) the volumetric bias for the calibration period.

Finally, the best 150 optimised parameter sets were retained for each catchment, subject to the constraint that the Nash–Sutcliffe values for all of the parameter sets for the validation period differ by no more than 2% for a given catchment. For parameter sets with identical Nash–Sutcliffe validation values, model performance was further discriminated based on the volumetric bias for the validation period.

The three-step procedure used for the selection and optimisation of hydrological model parameter sets, ensures that both (1) a large portion of the parameter space is sampled, thus overcoming the limitation of the local optimisation scheme used in PEST; and (2) the computationally intensive parameter optimisation procedure produces a

final set of model parameter sets with similar model fits, as judged by the Nash–Sutcliffe value for the validation period. Further details regarding the procedure used for HBV model calibration with PEST routines, as applied to 115 catchments throughout Norway, can be found in Lawrence *et al.* (2009).

The final validation Nash–Sutcliffe values for the optimised parameter sets for model validation vary somewhat between catchments (Flaksvatn, 0.78–0.80; Masi, 0.84–0.86; Nybergsund, 0.88–0.90; and Viksvatn, 0.86–0.88). The average model biases for the catchments are 1.1%, 1.2%, −2.0% and −2.4%, for Flaksvatn, Masi, Nybergsund and Viksvatn, respectively. Example fits based on a single parameter set for the year 1981 are illustrated in Figure 2 and indicate generally good model performance in simulating the highest flows during the year. In some cases, the flood recession periods following the highest flows and the low flow periods are not so well reproduced, but these shortcomings should not have an undue influence on the analysis of the average annual maximum runoff based on the simulated daily flows. Figure 2 also demonstrates quite effectively differences in the annual flow regimes in the catchments, with spring high flows dominating in Masi and, to some degree, in Nybergsund. Flaksvatn and Viksvatn experience high flows during the spring snowmelt period and in the autumn and early winter period due to high rainfall. In general, the highest flow during the snowmelt period tends to be better simulated than do the autumn and winter high flows, which are associated with more rapid rises and recessions. In some cases, the maximum flow values during autumn high flow events are underestimated by the model, highlighting a possible weaker model performance

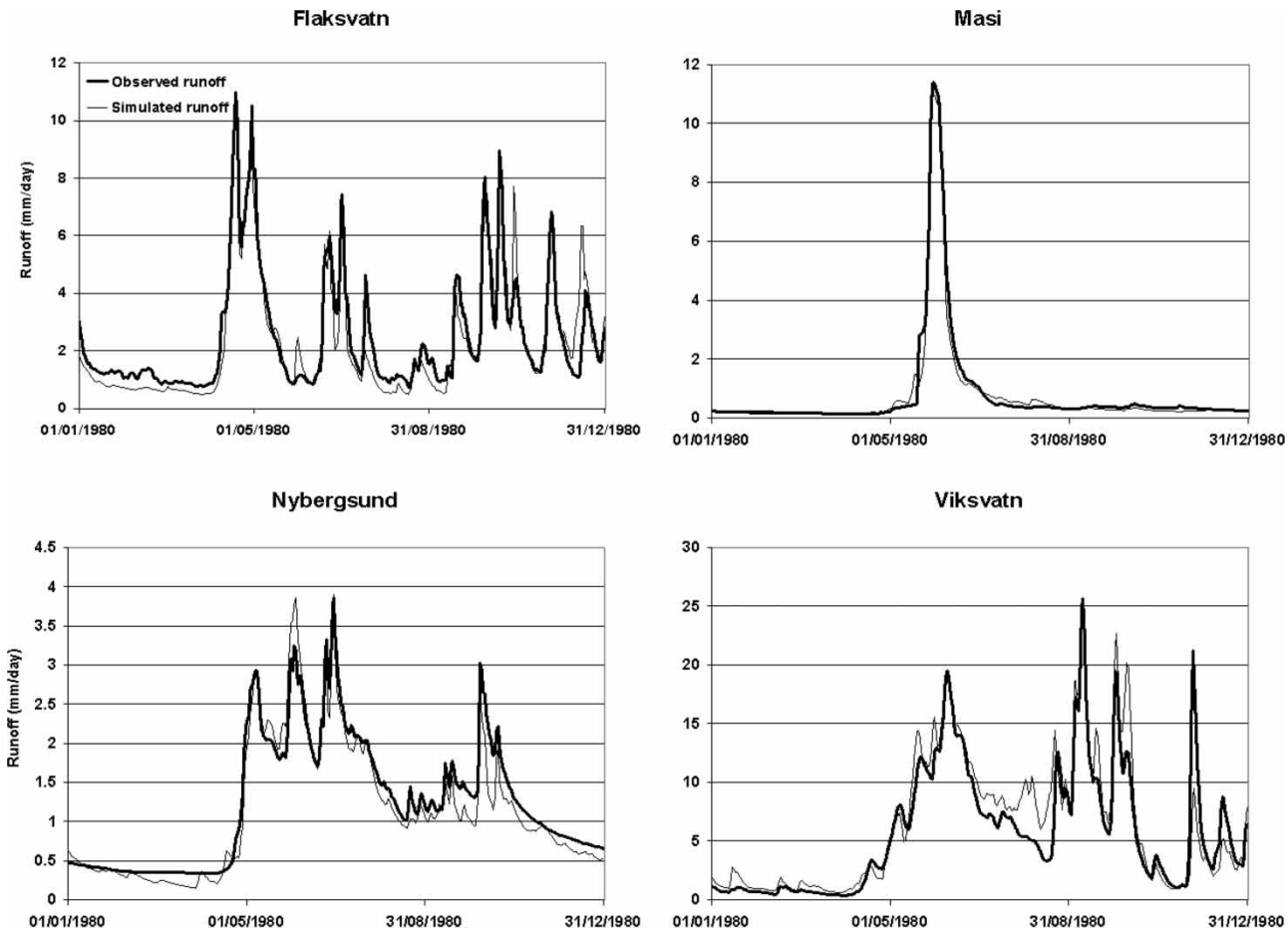

Figure 2 | Example model fit in each catchment for the calendar year 1980.

with respect to the assessment of high flows during these seasons.

PEST routines also generate information on parameter sensitivity during model optimisation. The most sensitive parameter varied between the catchments and between models for each catchment. The most sensitive parameters in Flaksvatn and Viksvatn models are KLZ (lower zone recession constant) and PKORR (rainfall correction factor). The snowfall correction factor (SKORR) and precipitation lapse rate (PGRD) also exhibited some sensitivity in these catchments. In Masi and Nybergsund, PKORR dominates model sensitivity and SKORR was the second most sensitive parameter, with KLZ also exhibiting some sensitivity. The dominance of PKORR, SKORR and KLZ in parameter sensitivity in these four catchments is consistent with HBV model calibrations for 115 catchments distributed throughout Norway (Lawrence *et al*. 2009). The sensitivity of the precipitation and snow correction factors is not surprising, in that this simply points to the fact that if one alters the input precipitation values, the simulated runoff will be altered. In other words, the model output is very responsive to the input values driving the hydrological model, and a small scaling of these values can have a significant effect on the modelled runoff. However, if the calibrated values for PKORR and SKORR differ significantly from 1.0, this implies that a correction of the input precipitation values leads to better model performance. The need for such a correction can be due to several factors, most notably the sparsity and lack of representativeness of the precipitation stations providing input data for the model. This lack of representativeness can be very pronounced in steep terrain, as precipitation stations tend to be located at lower elevations within a catchment and thus do not sample the highest elevations. In general, calibrated model parameter values for PKORR tended to be up to 10% less than 1.0, whilst values for SKORR tended to be greater than 1 (up to 20%). Co-variation of these two parameters suggests that in further model calibrations, they should be treated as 'linked parameters'. The third model parameter which was found to exhibit a high sensitivity, KLZ, controls the longest timescale in the hydrologic response, and thus the long-term recession to baseflow. This parameter was found to have a higher sensitivity in the smaller, steeper Viksvatn and Flaksvatn catchments. The overall hydrologic response time is much more rapid in these catchments than in Masi and Nybergsund, so one might anticipate that the recession to baseflow is of less importance to the overall model fit in these flashier catchments. However, these catchments are also subjected to multiple high flow events throughout the autumn and early winter periods, and the best model fits should reproduce a return to near baseflow following each of these periods (Figure 2). The occurrence of multiple high flows is, accordingly, a possible reason for the sensitivity of the KLZ parameter in these catchments.

Climate change scenarios

The scenario precipitation and temperature series of climate change impacts used here are based on RCM scenarios generated in the RegClim (Regional Climate Development under Global Warming) project (Bjørge *et al*. 2000) funded by the Norwegian Research Council. In that project, the HIRHAM regional climate model (Christensen *et al*. 1996) was applied to dynamically downscale simulations from two global climate models, ECHAM/OPYC3 (Roeckner *et al*. 1999) and HadAM3H (Pope *et al*. 2000). The ECHAM/OPYC3 model represents a coupling of the ECHAM4 atmospheric circulation model with the OPYC3 ocean circulation model, both of which were developed at the Max Planck Institute in Hamburg. The grid cell size is 2.8° by 2.8° (corresponding to 300 to 500 km, varying with latitute). The HadAM3H is a an atmospheric circulation model developed at the Hadley Centre in the United Kingdom. The spatial resolution of this global model is, however, higher, with grid cells corresponding to 1.875° longitude and 1.25° latitude. Output for model runs of the ECHAM/OPYC3 model are available for the IPCC SRES (Intergovernmental Panel on Climate Change Special Report on Emission Scenarios) B2 emissions scenario. The B2 SRES emissions scenario projects a 'moderate' level of greenhouse gas emissions by the end of the twenty-first century (see Watson (2001) for further details regarding IPCC SRES emissions scenarios). For the HadAM3H model, output from model runs are available for both the B2 and the A2 SRES emissions scenario, with the A2 scenario representing a 'high' level of greenhouse gas emissions by the end of the twenty-first century. Because the spatial resolution associated with the GCM applications is so coarse, the

model output is unsuitable for climate change impact analyses at a regional scale. The HIRHAM RCM was therefore used in the RegClim project to generate regional climate projections for a domain covering a large part of the Nordic region, at a spatial resolution of 55×55 km. These HIRHAM model runs use output from the ECHAM/OPYC3 (B2), HadAM3H (B2), and HadAM3H (A2) global climate model runs as model boundary conditions and thus generate dynamically downscaled climate model results at a spatial resolution of 55×55 km.

Precipitation and temperature series available from HIRHAM RCM application in the RegClim project, are however, still too coarse to be suitable for hydrological modelling at the scale of the catchments considered here (Table 1). This is particularly due to the smoothing of local topography which characterises the representation of surface elevation found in the RCM model grids. Therefore, the three scenarios available from the RegClim project were further adjusted using observed precipitation and temperature data from meteorological station sites in previous work by Beldring *et al.* (2008). Two approaches were applied: the delta change method (Reynard *et al.* 2001) and an empirical adjustment technique (Engen-Skaugen 2007). The delta change method is based on estimates of projected changes in relevant climate variables derived by comparing their values during a control period and a future period. These 'change factors' are then directly applied to an observed data time series. For the input time series used in this work (and reported in Beldring *et al.* 2008), changes in monthly temperature and precipitation between a 1961–1990 control period and a 2071–2100 future period were estimated from the RCM output and applied to the daily station temperature and precipitation time series for the control period. This method is simple to implement and has been widely applied in climate impact research. It does not, however, provide a direct coupling with the daily RCM output. Accordingly, important changes, for example in the standard deviation of precipitation values, are not necessarily transferred from the climate model output to the locally adjusted data with this method. The 'empirical adjustment' technique, alternatively, refines the daily RCM output to better reflect local conditions. RCM output for temperature is height corrected for individual stations, and output for precipitation during a control period is corrected relative to observed monthly data. Further empirical adjustment of both precipitation and temperature are applied to RCM output for the future scenario period, based on residuals representing the variability of daily precipitation or temperature. The method preserves the relative changes in mean values and in the standard deviation based on daily values, between the control and future periods, as simulated by the RCM. The empirical adjustment method was applied to the output time series from the RCM scenarios for the one or more grid cells corresponding to particular precipitation and temperature stations.

Following the application of methods for adjusting the RCM output to a local scale, six projected temperature and precipitation series for the period 2071–2100, together representing two GCMs, two emission scenarios and two methods for local adjustment, were available for simulating runoff under a future climate. In order to assess likely hydrological changes under a future climate, a comparison must be made with present-day conditions. It is not, however, appropriate to compare simulated daily runoff under a future climate directly with observed runoff data from a historical period, due to potential biases introduced by the hydrological and the climate models. For the scenario data generated using the delta change method, comparisons can be made directly with modelled runoff data for a historical reference period, for which observed temperature and precipitation are used as an input data for the hydrological modelling. For scenarios generated directly from daily RCM output using the empirical adjustment method, comparisons are, alternatively, made with hydrological simulations for the reference period using the adjusted RCM temperature and precipitation series for that period. For the climate change scenarios considered in this work, the period 1961–1990 represents the reference period. Three input data series for hydrological modelling of runoff during the reference period were used in this work: (1) observed temperature and precipitation data for simulating runoff suitable for comparison with runoff simulated using the future scenario data adjusted using the delta change technque; (2) the empirically adjusted precipitation and temperature series from the RCM runs based on the HadAM3H model (hereafter referred to as the Hadley model) runs for comparison with runoff simulated for the future period using the empirically adjusted Hadley model

output; and (3) the empirically adjusted precipitation and temperature series from the RCM runs based on the ECHAM/OPYC3 model (hereafter referred to as the ECHAM model) runs for comparison with runoff simulated for the future period using the empirically adjusted ECHAM model output.

The HBV model was run for each of the nine input time series, described in the two previous paragraphs, for each catchment for each of the 150 parameter sets validated for that catchment. Each modelled daily time series was then analysed to identify the maximum daily runoff for each of the 30 years represented by the simulated series, and an average value of this quantity was calculated for the series. Empirical cumulative probability functions representing the distribution of all of the values of the average annual maximum daily mean runoff were then constructed for each catchment for particular scenarios and for the combined results of all of the future scenarios.

ANALYSIS AND RESULTS

The cumulative distribution functions for the modelled average annual maximum daily mean runoff for the reference period scenarios (1961–1990) and for the combined distribution for all six future period runs (2071–2100) are illustrated in Figure 3 for the four catchments. The 'Observed *P*, *T*' function represents the distribution of model results based on the observed precipitation and temperature during the reference period (1961–1990) as input to all HBV parameter sets for a given catchment. Similarly, the functions for the individual Hadley and ECHAM control runs are illustrated. The diagrams illustrate the 5% to 95% range for each of these sets of model results. For each of the three functions 'Observed *P*, *T*', 'Hadley (1961–1990)' and 'ECHAM (1961–1990)', the range of values for an individual function gives an indication of the uncertainty introduced by the model parameter sets (i.e. hydrological model uncertainty). In three of the catchments, Flaksvatn, Nybergsund and Masi, the reference period run for the ECHAM model more closely reproduces results simulated from the observed *P*, *T* values than does the Hadley model. In Viksvatn, however, the Hadley model output more is more similar to that derived from observed climate data, although the differences between the ECHAM and Hadley model are small. The largest difference between the climate model reference period runs and the runs based on observed climate data are seen in Flaksvatn, where the Hadley model produces higher values for the modelled average maximum daily flow than those modelled based on observed input data. If these results were to be used as absolute values, for example, in the design of structures or the analysis of dam safety, then it would be appropriate to bias correct the modelled runoff with observed runoff values. However, as the analysis here is concerned with percentage changes in runoff between two time periods, such a correction would be of no consequence and so has not been undertaken.

The combined cumulative distribution functions for all model runs based on climate scenario input data for the future period (2071–2100) are also illustrated in Figure 3. The irregularity of the functions shown for Masi and Nybergsund reflect the combination of discrete, non-overlapping sets of model results derived from the differing climate models. For the future period, the climate model scenario data produce divergent results in these two catchments. In all cases, however, the 5% to 95% range illustrated for the future period is distinct from and non-overlapping with the distributions for the reference period. Comparison of the reference period and the future period functions indicate projected increases in the average annual maximum mean daily runoff in Flaksvatn and Viksvatn and decreases in Masi and Nybergsund. These general trends are consistent with previous analysis of projected seasonal changes in runoff in these catchments (Beldring *et al*. 2006).

The results illustrated in Figure 3 can be further quantified based on the difference between the median values for the reference period and the future period cumulative distribution functions. Accordingly, a combined cumulative distribution function was constructed based on the two reference period runs illustrated in Figure 3. The difference between the median values for this function and the 'All scenarios (2071–2100)' function illustrated in Figure 3 was then calculated. The estimated projected changes in the average annual maximum daily mean flow in each of the four catchments are illustrated in Figure 4 and are given as a percentage of the average annual maximum daily flow calculated from the reference period. The range of results,

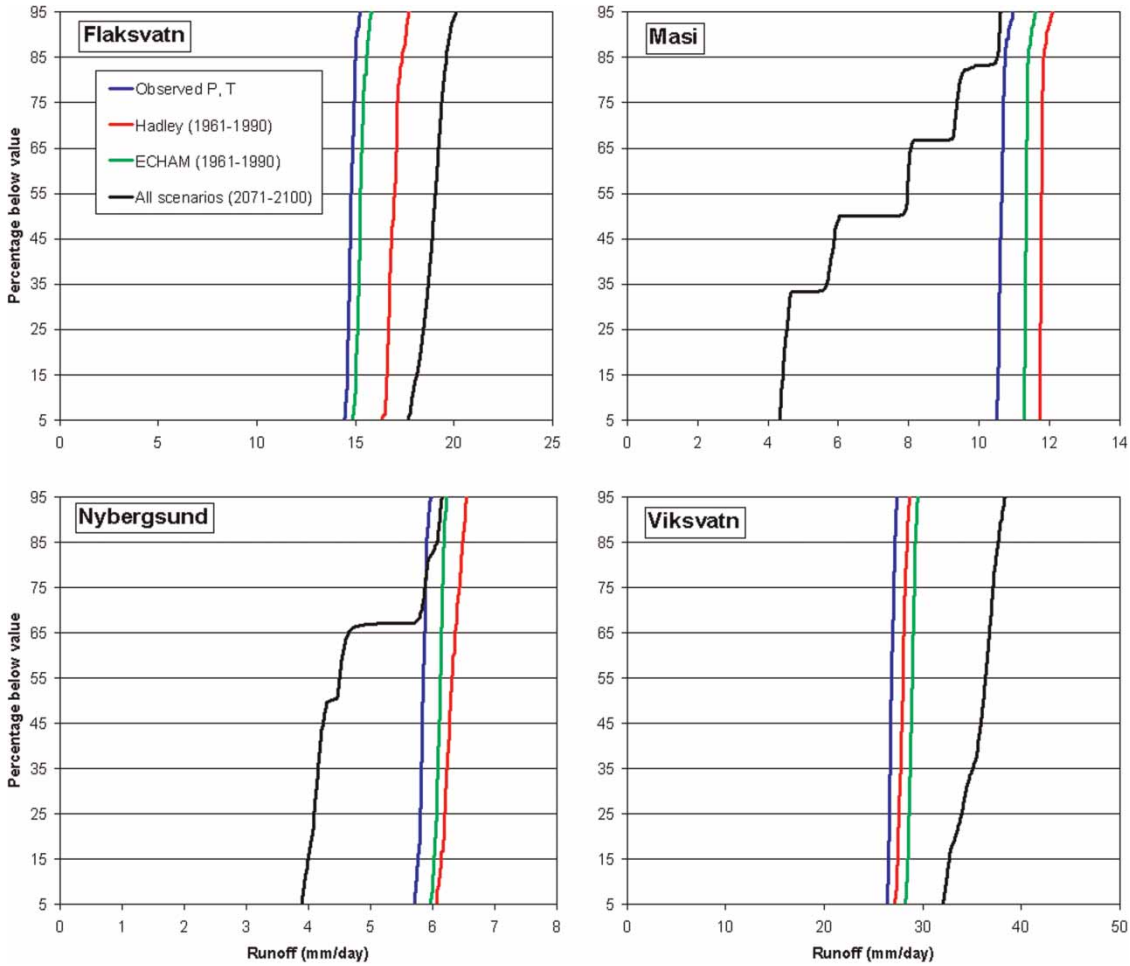

Figure 3 | Cumulative distribution functions for the combined results for the models based on the input precipitation and temperature series indicated.

based on the difference between the reference period 5th and 95th percentile values and the 'All scenarios (2071–2100)' values are also illustrated. Figure 4 illustrates both differences in the magnitude and direction of anticipated changes and in the uncertainty range underlying those projections, as estimated from the models considered here. In particular, the projections for catchments located in areas where the highest annual flows are generated by snowmelt flooding (Masi and Nybergsund) are associated with larger uncertainty ranges than catchments in western and southern Norway, where the rainfall flooding is expected to become increasing dominant in the generation of the highest flows during a given year.

The relative importance of various factors contributing to the range of results illustrated in Figure 4 can be estimated from cumulative distribution functions partitioned to isolate individual sources of uncertainty. Such functions are illustrated in Figure 5 for Flaksvatn for the greenhouse gas emissions scenario (A2 versus B2), the global climate model (ECHAM versus Hadley) and the local adjustment method (delta change *vs*. empirical adjustment). The distribution functions in Figure 5 are constructed using a resampling of all model results to construct functions representing the factor indicated. These plots illustrate, for example, that differences in model results obtained from different emission scenarios and local adjustment methods are larger than those associated with the use of the ECHAM versus the Hadley global climate models in Flaksvatn. Figure 6 illustrates the range of model results for individual input data sets, thus displaying the uncertainty

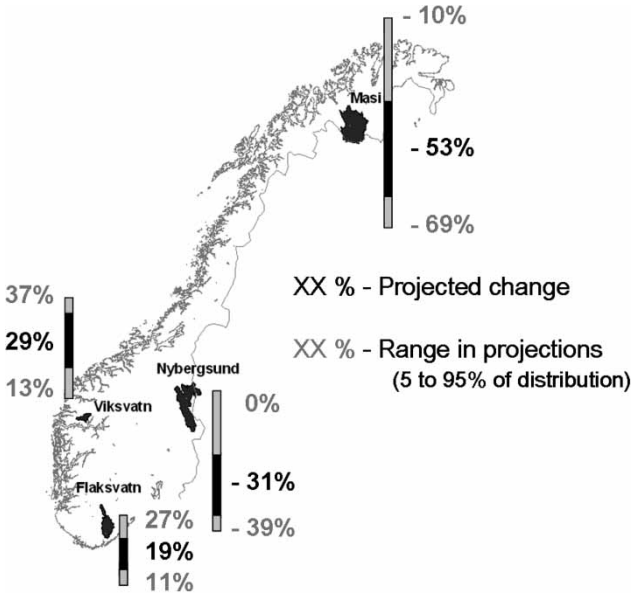

Figure 4 | Projected changes in the average annual maximum daily mean runoff between the reference period (1961–1990) and the future period (2071–2100) for the modelled catchments.

derived from HBV model parameterisation, relative to the differences between individual input datasets. The distribution function constructed from the results for the modelled observed *P*, *T* input data exhibits a range (~5%) which is greater than the 2% range in fits for the calibrated parameter sets. This arises due to the use of the Nash–Sutcliffe value, which is a measure of overall fit for the entire time series, as the primary calibration criterion, rather than a criterion which specifically tests model fit with respect to the highest flows during each year. The range of results is also larger for the modelled future scenarios, ranging from ~7% to 15%, indicating that uncertainty derived from HBV parameterisation increases when input data derived from future climate scenarios are used.

The distribution functions illustrated in Figures 5 and 6 were used to estimate the differences between the individual functions representing single uncertainty sources, and these are given in Table 3. For three of these sources, the emission scenario, the GCM and the local adjustment technique, the difference reported has been calculated as the average absolute difference between the two functions over the 5 to 95% range. This is used, rather than simply estimating the difference in the median values, in order to account for the dissimilar shapes of the two curves. For the HBV parameter

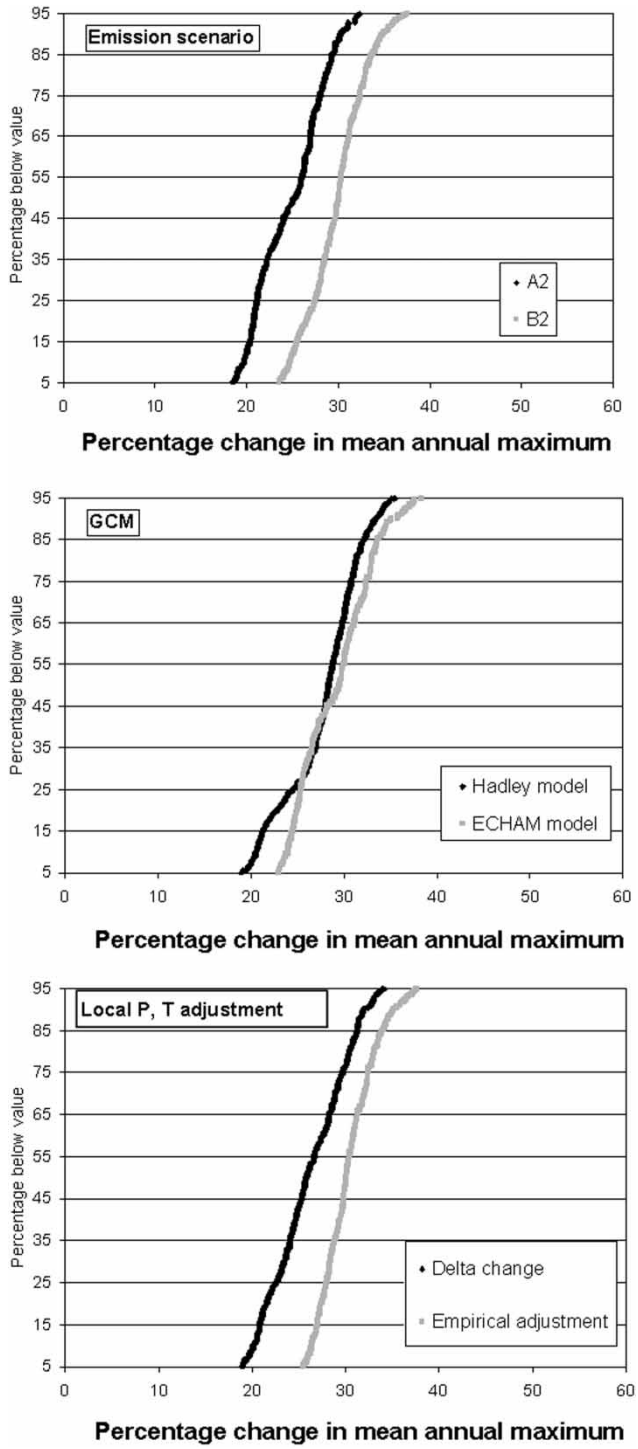

Figure 5 | Cumulative distribution functions for Flaksvatn for the combined results for the variable indicated.

uncertainty, the value reported represents the median value for the 5–95% ranges for all of the future scenarios, as shown

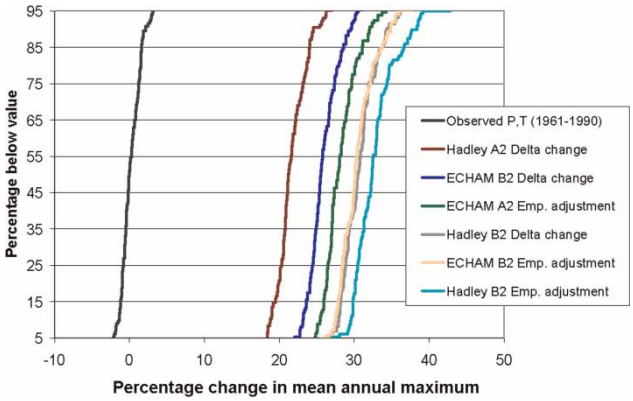

Figure 6 | Cumulative distribution functions for Flaksvatn for the results from individual input dataseries.

in Figure 5. The absolute values for these quantities and the percentage contribution (i.e. the relative contribution) to the sum of all uncertainty sources for each catchment are given.

The results given in Table 3 illustrate considerable differences in the contributions of individual factors to uncertainty in the results for the four catchments. The generally larger absolute values associated with Masi and Nybergsund reflect the wider range in the results, as illustrated in Figure 4 for these catchments. The local adjustment method makes the largest relative contribution to uncertainty in Masi and Nybergsund, whilst differences between the GCMs and between emission scenarios are also large. The relative magnitude of the range attributed to HBV model parameter uncertainty indicates that it is of less relative importance in Masi and Nybergsund, both when compared with other factors in these catchments and with HBV parameter uncertainty in Flaksvatn and Viksvatn. Flaksvatn is associated with the largest contribution from HBV model parameter uncertainty, both relative to other factors for this catchment, and with respect to parameter uncertainty in other catchments. Viksvatn exhibits larger parameter uncertainty than Masi and Nybergsund, but the contribution of differences between emission scenarios and GCMs is larger in Viksvatn than is HBV model parameter uncertainty.

Table 3 | Contribution of the four sources of model uncertainty to range of ensemble results

Uncertainty source	Flaksvatn	Masi	Nybergsund	Viksvatn
Emissions scenario	5 (25%)	9 (13%)	9 (17%)	14 (41%)
Global climate model	2 (10%)	16 (23%)	14 (27%)	10 (29%)
Local adjustment method	4 (20%)	42 (60%)	25 (48%)	3 (9%)
HBV parameterisation	9 (45%)	3 (4%)	4 (8%)	7 (21%)

DISCUSSION

The results of the ensemble modelling of climate change impacts on the average annual maximum daily mean runoff indicate a considerable degree of variability in the range of outcomes and in the contribution of climate scenario input data versus HBV model parameter sets to this range in the four catchments considered. Although differences between results derived from various global climate models and greenhouse gas emission scenarios or downscaled using alternative techniques are expected and have been reported in previous work (e.g. Beldring *et al.* 2008), the relative contribution of HBV parameter uncertainty merits further discussion. In Masi and Nybergsund, the magnitude of HBV parameter uncertainty is of less importance than other factors, although this factor dominates uncertainty in the Flaksvatn results and is of a similar magnitude to other factors in Viksvatn. The overall model fits attained in Flaksvatn are slightly weaker (0.78–0.80) than in the other catchments and this is a likely contributing factor to the larger spread in results based on future climate data. However, this does not fully explain the differences seen when Viksvatn is compared with Masi and Nybergsund, with the parameter sets for Viksvatn (0.86–0.88) exhibiting generally better model fits than Masi (0.84–0.86). An additional factor that may contribute to differences in model performance is the overall range of parameter values found in the calibrated model parameter sets for each catchment, given in Table 4. The largest and second largest parameter ranges for each calibrated HBV parameter are indicated in bold in Table 4, illustrating that most of the larger ranges are found in the sets of calibrated models for Flaksvatn and Viksvatn. So, although model fits to the time series used for calibration are good to very good in these catchments, the underlying models represent a wider selection of the available parameter values than

Table 4 | Range of calibrated HBV parameters by catchment

HBV Parameter	Total range available during calibration	Range of calibrated parameter sets			
		Flaksvatn	Masi	Nybergsund	Viksvatn
BETA	3.0	**2.6**	1.61	0.35	**3**
CX	4.0	**2.19**	1.37	1.59	**2.69**
FC	450.0	**450**	86.68	292.84	**375.55**
KLZ	0.099	**0.08**	**0.02**	0.005	0.016
KUZ1	0.99	**0.14**	0.05	0.03	**0.17**
KUZ2	0.9	**0.38**	0.1	0.07	0.1
PERC	1.5	**1.41**	1.35	0.83	**1.5**
PGRD	0.1	**0.1**	0.06	0.06	**0.1**
PKORR	2.2	**0.15**	0.1	**0.11**	0.1
SKORR	2.0	0.04	**0.33**	0.01	**0.2**
TS	3.0	**1.59**	1.14	1.42	**2.81**
TX	3.0	2.37	2.74	**2.95**	**2.75**
TTGD	0.5	**0.46**	0.11	**0.5**	0.31
TVGD	0.4	0.35	**0.38**	0.37	**0.40**
UZ1	90	40.22	24.67	**51.86**	**89.43**

those calibrated for Masi and Nybergsund. In other words, these calibrated model sets for Flaksvatn and Viksvatn are not as well constrained, thus providing scope for a broader range of outcomes when input data are perturbed.

From a physical perspective, it is also notable that the dominant high flow generating mechanism under a future climate also differs between the two sets of catchments. In Masi and Nybergsund, high flows will most likely continue to be associated with spring snowmelt, although such flows are expected to occur earlier and with a reduced volume. Figure 2 also suggests that Nybergsund is perhaps somewhat more vulnerable to future increases in rainfall-induced high flows during the autumn, if this particular year is taken to be representative of the annual flow regime. In both Flaksvatn and Viksvatn, rainfall flooding is projected to become increasingly dominant in the generation of annual high flows. Increased rainfall flooding in Flaksvatn and Viksvatn is also associated with a shift in seasonality, such that high flows should more often be associated with autumn and winter periods. Thus, with reference to Figure 2, the highest flows in these catchments will increasingly be associated with periods during the year in which the model performance during the calibration period is somewhat more erratic. These changes in the dominant flood generation mechanism and in seasonality may also contribute to the increased HBV model parameter uncertainty found in the distribution functions for future scenarios for Flaksvatn and Viksvatn.

The approach presented here is based on an equal weighting for the six 2071–2100 climate scenario datasets and provides an indication of the relative significance of HBV model parameter uncertainty given an ensemble of future climate input time series for model forcing in the four catchments considered. The results illustrated should not, however, be interpreted as a full quantification of the uncertainties for several reasons. First, the range of the input time series representing different GCMs and emission scenarios has been limited by the availability of locally adjusted climate scenario data suitable for catchment-scale modelling. This range will be expanded as additional series become available for these catchments and may result in a higher proportion of the total uncertainty being due to differences between GCMs. However, some GCMs perform better than others for particular catchments (e.g. Figure 2) and also for particular flow indices. The inclusion of time series derived from additional GCM and RCM model runs is, therefore, probably best pursued using weightings for individual scenarios based on their skill in reproducing a particular flow index of interest in a reference period (e.g. Wilby & Harris 2006), rather than introducing the widest possible range of scenarios using equal weightings. Second, model structure has not been considered here, but would be expected to contribute to uncertainty in hydrological projections for a future climate. The increase in the range of HBV parameter uncertainty between the control and the future period itself raises questions as to the overall robustness of a calibrated HBV model when applied beyond the range of climatic conditions for which it was developed. Additionally, previous work (Andréasson *et al*. 2004) indicates that, in particular, the temperature-index approach used for calculating evapotranspiration in HBV overestimates future increases in evaporatranspiration relative to that given by climate models. Uncertainty associated with the simplified evapotranspiration routine used in HBV is, in general, likely to be significant and has not been considered in this application. This application has, however, focused particularly on percentage changes in the highest

annual flows, occurring either during the spring snowmelt period or in the autumn/early winter period. The influence of differences in methods for calculating evapotranspiration are not as significant in this case as they would be in an investigation of droughts, for example, or of seasonal volumes. Finally, the role of natural variability has not been included here, but could be investigated in conjunction with the application of weather generators (e.g. Fowler *et al.* 2007; Minville *et al.* 2008) to produce multiple realisations of each downscaled scenario as input to the hydrological model. Such an approach would allow a further comparison to be drawn between the uncertainty sources evaluated here relative to modelled variability in the input data series.

CONCLUSIONS

The analysis and results presented in Figures 3–6 illustrate a simple methodology for evaluating and displaying the range of results from a climate impact analysis derived from multiple hydrological projections. As the results are given in the form of probability distribution functions for the outcomes, the likelihood of a change of a given magnitude can be estimated and further used, for example, in risk assessment. Such an approach can be applied in the analysis of increased future flood risks in conjunction with flood risk management or in the assessment of dam safety under a future climate. The probability of changes in seasonal runoff of a given magnitude is also of interest in assessing future hydropower production potential and could be evaluated with such an approach. The results of this type of quantitative analysis are, however, dependent on the selection of models used for generating the ensemble of projections, and this should be carefully considered in the application of such a methodology. A contribution of this approach to that selection process is that it can be used to quantify the significance of various alternative assumptions or models to the range of ensemble results. The example presented here also demonstrates the high degree of variability in the principal sources of uncertainty in the hydrological projections for the four catchments considered. Further work is considering this issue based on 115 catchments of varying size distributed throughout Norway (i.e. Lawrence and Engen-Skaugen 2010; Lawrence 2010), and the results will be used to identify areas most likely to be subjected to an increased flood risk under a future climate.

ACKNOWLEDGEMENTS

The study presented here is funded in part by Nordic Energy Research within the 'Climate and Energy Systems' project, by the NORKLIMA programme of the Research Council of Norway through the 'CELECT (Climate change impacts in the electricity sector)' project, and the EU Interreg IV 'SAWA (Strategic Alliance for Water Management Actions)' project. We also thank two anonymous reviewers and the editor for their detailed comments which have significantly improved the manuscript.

REFERENCES

Andréasson, J., Bergström, S., Carlsson, B., Graham, L. P. & Lindström, G. 2004 Hydrological change – Climate change impact simulations for Sweden. *Ambio* **33**, 228–234.

Arnell, N. W. 1999 The effect of climate change on hydrological regimes in Europe: a continental perspective. *Global Env. Change* **9**, 5–23.

Beldring, S., Engeland, K., Roald, L. A., Sælthun, N. R. & Voksø, A. 2003 Estimation of parameters in a distributed precipitation-runoff model for Norway. *Hydrol. Earth Syst. Sci.* **7**, 304–316.

Beldring, S., Engen-Skaugen, T., Førland, E. & Roald, L. A. 2008 Climate change impacts on hydrological processes in Norway based on two methods for transferring regional climate model results to meteorological stations sites. *Tellus A – Dynam. Meteorol. Oceanograph.* **60**, 439–450.

Beldring, S., Roald, L. A., Engen-Skaugen, T. & Førland, E. 2006 *Climate Change Impacts on Hydrological Processes in Norway 2071–2100*. Norwegian Water Resources and Energy Directorate Report No 6-2006, Oslo.

Bergström, S. 1976 *Development and Application of a Conceptual Runoff Model for Scandinavian Catchments*. Swedish Meteorological and Hydrological Institute Report RH07, Norrköping.

Bergström, S. 1995. The HBV model. In: *Computer Models of Watershed Hydrology* (V. P. Singh, ed.). Water Resources Publications, Highlands Ranch, pp. 443–476.

Bergström, S., Carlsson, B., Gardelin, M., Lindström, G., Pettersson, A. & Rummukainen, M. 2001 Climate change impacts on runoff in Sweden – assessments by global climate models, dynamical downscaling and hydrological modelling. *Clim. Res.* **16**, 101–112.

Bjørge, D., Haugen, J. E. & Nordeng, T. E. 2000 *Future Climate in Norway. Dynamical Downscaling Experiments within the RegClim Project*. Research Report no. 103. Norwegian Meteorological Institute.

Christensen, J. H., Bøssing Christensen, O., Lopez, P., van Meijgaard, E. & Botzet, M. 1996 *The HIRHAM4 Regional Atmospheric Climate Model*. Scientific Report 96-4, Danish Meteorological Institute.

Diaz-Nieto, J. & Wilby, R. L. 2005 A comparison of statistical downscaling and climate change factor methods: impacts on low-flows in the river Thames, United Kingdom. *Clim. Change* **69**, 245–268.

Doherty, J. 2004 PEST. *Model Independent Parameter Estimation*. Fifth edition of user manual. Watermark Numerical Computing, Brisbane, Australia.

Engen-Skaugen, T. 2007 Refinement of dynamically downscaled precipitation and temperature scenarios. *Clim. Change* **84**, 365–382.

Fowler, H. J., Blenkinsop, S. & Tebaldi, C. 2007 Linking climate change modelling to impacts studies: recent advances in downscaling techniques for hydrological modelling. *Int. J. Climatol.* **27**, 1547–1578.

Graham, L. P., Andréasson, J. & Carlsson, B. 2007 Assessing climate change impacts on hydrology from an ensemble of regional climate models, model scales and linking methods – A case study on the Lule River basin. *Clim. Change* **81** (Suppl.), 293–307.

Kite, G. W. & Kouwen, N. 1992 Watershed modelling using land classifications. *Water Res. Res.* **28**, 3193–3200.

Kriaučiūnienė, J., Šarauskienė, D. & Gailiušis, G. 2009 Estimation of uncertainty in catchment-scale modeling of climate change impact (Case of the Merkys River, Lithuania). *Env. Res. Engng Manag.* **1** (47), 30–39.

Lawrence, D. 2010 Hydrological projections for changes in flood frequency under a future climate in Norway and their uncertainties. In: *Hydrology: From Research to Water Management* (E. Apsite, A. Briede & M. Klavins, eds.), Proceedings of the XXVI NHC, NHP Report No. 51, 203–204.

Lawrence, D. & Engen-Skaugen, T. 2010 Floods in Norway under a near future 2021–2050 climate: hydrological projections for rainfall vs. snowmelt floods and their uncertainties. In *Proceedings of the Conference on Future Climate and Renewable Energy: Impacts, Risks and Adaptation, 31 May–2 June 2010*. Norwegian Water Resources and Energy Directorate, Oslo, pp. 32–33.

Lawrence, D., Haddeland, I. & Langsholt, E. 2009 *Calibration of HBV Hydrological Models using PEST Parameter Estimation*. NVE Report No. 1.

Lindström, G., Johansson, B., Persson, M., Gardelin, M. & Bergström, S. 1997 Development and test of the distributed HBV-96 hydrological model. *J. Hydrol.* **201**, 272–288.

Minville, M., Brissette, F. & Leconte, R. 2008 Uncertainty of the impact of climate change on the hydrology of a nordic watershed. *J. Hydrol.* **358**, 70–83.

New, M. & Hulme, M. 2000 Representing uncertainty in climate change scenarios: a Monte Carlo approach. *Integr. Assess.* **1**, 203–213.

Petterson, L. E. 2004 Aktive Vannføringsstasjoner i Norge. NVE Rapport nr 16.

Pope, V. D., Gallani, M. L., Rowntree, P. R. & Stratton, R. A. 2000 The impact of new physical parameterisations in the Hadley Centre model: HadAM3. *Clim. Dynam.* **16**, 123–146.

Prudhomme, C., Jakob, D. & Svensson, C. 2003 Uncertainty and climate change impact on the flood regime of small UK catchments. *J. Hydrol.* **277**, 1–23.

Reynard, N. S., Prudhomme, C. & Crooks, S. M. 2001 The flood characteristics of large UK rivers: potential effects of changing climate and land use. *Clim. Change* **48**, 343–359.

Roeckner, E., Bengtsson, L., Feichter, J., Lelieveld, J. & Rodhe, H. 1999 Transient climate change simulations with a coupled atmospheric-ocean GCM including the tropospheric sulfur cycle. *J. Climate* **12**, 3004–3032.

Sælthun, N. R. 1996 *The Nordic HBV Model*. Norwegian Water Resources and Energy Administration, Publication 7, Oslo.

Salathé, E. P. 2003 Comparison of various precipitation downscaling methods for the simulation of streamflow in a rainshadow river basin. *Int. J. Climatol.* **23**, 887–901.

Salathé, E. P. 2005 Downscaling simulations of future global climate with application to hydrologic modelling. *Int. J. Climatol.* **25**, 419–436.

Schaefli, B., Hingray, B. & Musy, A. 2007 Climate change and hydropower production in the Swiss Alps: quantification of potential impacts and related modelling uncertainties. *Hydrol. Earth Syst. Sci.* **11**, 1191–1205.

Skahill, B. E. & Doherty, J. 2006 Efficient accommodation of local minima in watershed model calibration. *J. Hydrol.* **329**, 122–139.

Solomatine, D. P., Dibike, Y. B. & Kukuric, N. 1999 Automatic calibration of groundwater models using global optimization techniques. *Hydrol. Sci. J.* **44**, 879–894

Steele-Dunne, S., Lynch, P., McGrath, R., Semmler, T., Wang, S., Hanafin, J. & Nolan, P. 2008 The impacts of climate change on hydrology in Ireland. *J. Hydrol.* **356**, 28–45.

Watson, R. T. 2001 *Climate Change 2001: Synthesis Report*. A contribution of working groups I, II and III to the Third Assessment report of the Intergovernmental Panel on Climate Change, Cambridge University Press, Cambridge.

Wilby, R. A. & Harris, I. 2006 A framework for assessing uncertainties in climate change impacts. *Water Res. Res.* **42**, W02419.

Wood, A. W., Leung, L. R., Sridhar, V. & Lettenmaier, D. P. 2004 Hydrologic implications of dynamical and statistical approaches to downscaling climate model outputs. *Clim. Change* **62**, 189–216.

First received 22 January 2009; accepted in revised form 20 September 2010. Available online July 2011